

## BUBBLE DIAMETER ON DETACHMENT IN FLOWING LIQUIDS

R. A. M. AL-HAYES and R. H. S. WINTERTON

Mechanical Engineering Department, Birmingham University,  
P.O. Box 363, Birmingham B15 2TT, U.K.

(Received 24 April 1980 and in revised form 4 July 1980)

**Abstract**—An extensive series of measurements of gas bubble diameters on detachment into flowing liquids has been performed. The test liquids were water, water with surface active agent, and ethylene glycol. By use of different surfaces equilibrium contact angles ranging from 22 to 90° were obtained. Based on these results new expressions are proposed for the surface tension and drag forces experienced by a bubble attached to a solid surface.

### NOMENCLATURE

$C_d$	drag coefficient;
$d$	bubble diameter;
$F_b$	buoyancy force on bubble;
$F_d$	drag force on bubble;
$F_s$	surface tension force on bubble;
$g$	acceleration due to gravity;
$r$	bubble radius;
$Re_b$	bubble Reynolds number, $\rho du/\mu$ ;
$u$	local flow velocity past bubble;
$\theta_a$	advancing contact angle;
$\theta_r$	receding contact angle;
$\theta_0$	equilibrium contact angle;
$\mu$	viscosity of liquid;
$\rho$	density of liquid;
$\sigma$	surface tension.

### INTRODUCTION

THE PREVIOUS paper described the mass transfer processes controlling the growth of gas bubbles attached to a solid surface. This paper is concerned with the maximum diameter the bubbles can reach before they are swept off into the flowing liquid.

The question of the size of gas bubbles that can adhere to heat transfer surfaces, and that can be swept off surfaces elsewhere in heat transfer equipment, has proved of significance in a number of fields. Previously unexplained reductions in liquid metal heat transfer have been interpreted on the assumption that there was a dense layer of gas bubbles adhering to the surface. The diameter of the bubbles varied with the surface conditions and the liquid flow rate [1, 2]. All the main trends evident in liquid metal superheat experiments may be explained on the assumption of nucleation by gas bubbles that have been swept off walls elsewhere in the system [3]. The point at which individual bubbles could become so large as to give local hot spots on the heat exchange surface has been shown to be consistent with fuel pins failures observed

in tests in an experimental nuclear reactor [4]. The basic theory for these calculations, together with a limited degree of experimental confirmation, has been given in [5].

Since this topic appeared to have received comparatively little systematic study, and in view of the numerous practical applications, it was felt desirable to extend the experimental measurements of [5] to a wider range of flow geometries, bubble contact angles and test liquids. Although these measurements involve the comparatively slow growth of gas bubbles, where inertial forces can be neglected, they will almost certainly provide insight into the forces acting on vapour bubbles in flow boiling.

### THEORY

The basis of the theoretical approach is that three distinct forces may act on the bubble: buoyancy, drag and surface tension. The bubble will detach from the surface into the flowing liquid if the resultant of the buoyancy and drag forces is greater than the surface tension force. This resolution of forces is conducted parallel to the surface, since the surface tension force in this direction arises from the difference in contact angle on the two sides of the bubble, and is much weaker than the surface tension force perpendicular to the surface.

The first two forces are calculated simply on the assumption that the bubble is a truncated sphere with a contact angle on the surface equal to the equilibrium contact angle  $\theta_0$ . The buoyancy force is

$$F_b = \rho g \frac{1}{3} \pi r^3 \{2 + 3 \cos \theta_0 - \cos^3 \theta_0\}.$$

The drag force is proportional to the projected area of the bubble facing the flow and the dynamic pressure of the coolant, i.e.

$$F_d = C_d \frac{1}{2} \rho u^2 r^2 \{\pi - \theta_0 + \cos \theta_0 \sin \theta_0\} \quad (1)$$

where  $C_d$  is the drag coefficient.  $u$  is calculated from the appropriate velocity profile at a distance equal to one

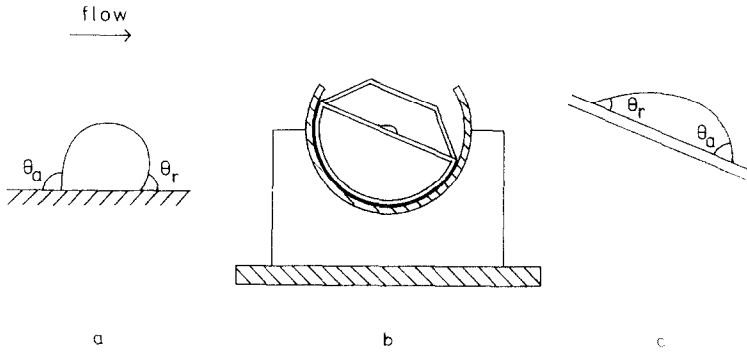


FIG. 1(a). Appearance of the bubble just before detachment. The contact angles (measured through the liquid) reach their limiting advancing and receding values. (b) Test cells used to measure the advancing and receding angles. (c) Close up view of drop of liquid in the test cell.

half the distance the bubble projects from the wall, i.e. at a distance  $r(1 + \cos \theta_0)/2$ . The usual velocity profile for a turbulent flow is used (e.g. [5], except that the correct logarithmic law is used in the buffer layer rather than the simpler power law). A parabolic profile is used for laminar flow.

Previously it has been assumed that the values of  $C_d$  for freely rising bubbles given in [6] could be used. In most cases this has meant  $C_d = 18.7/Re_b^{0.68}$ . This assumption has limited previous analyses to fairly small contact angles, where it might be reasonable to

regard the bubble attached to the wall as equivalent to a free bubble. For large contact angles of around  $90^\circ$  the bubble adhering to the wall is roughly a hemisphere, and it was not considered likely that the same drag coefficient could be used. Part of the intention behind the present project was to provide a sounder experimental basis for the calculation of  $C_d$ .

Under the influence of the buoyancy and drag forces the bubble shape distorts, the effect being as shown in Fig. 1(a) if the drag force dominates. The surface tension force acts along the line of contact between the bubble and the solid surface, and the contributions from opposite sides of the bubble, resolved along the

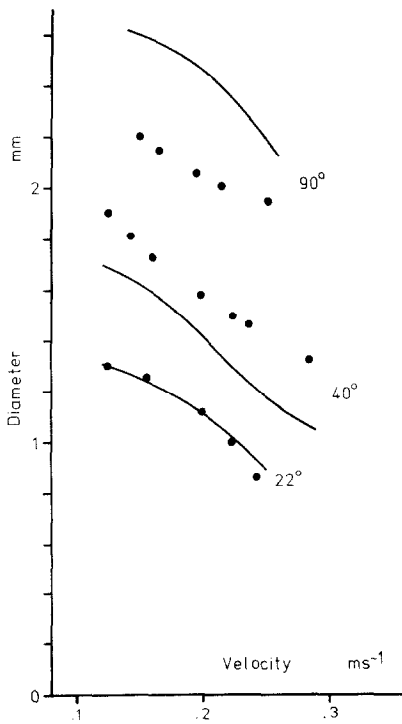


FIG. 2. Bubble diameter on detachment for horizontal flow of water in the 19 mm tubes. The continuous curves are the final theoretical predictions using the measured contact angles. The contact angles, in the order equilibrium, advancing, and receding, were: 90, 100, 80; 40, 30, 50; and 22, 34, 10.

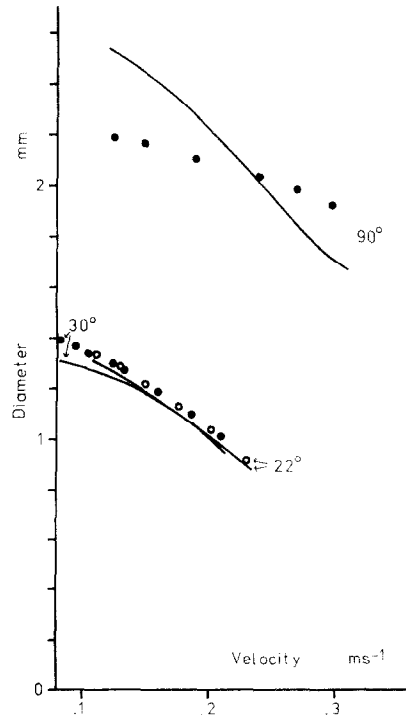


FIG. 3. Results for upward flow of water in the 23 mm tubes. The contact angles were: 90, 100, 80; 30, 38, 22; and 22, 34, 10.

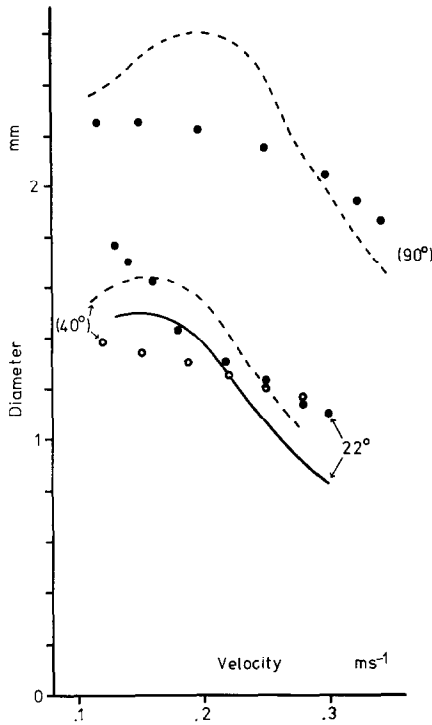


FIG. 4. Results for downward flow of water in the 19 mm tubes. The measured contact angles were: 90, 100, 80; 40, 30, 50; and 22, 34, 10. To obtain the dashed curves it was necessary to bring both advancing and receding contact angles  $2^\circ$  closer to the equilibrium value.

surface, tend to cancel out. They do not cancel completely however since the contact angle is not the same on the upstream and downstream sides. It is well known that small variations in contact angle are observed depending on whether the liquid is advancing or receding from the solid surface. The limiting values of these angles are known simply as the advancing ( $\theta_a$ ) and receding ( $\theta_r$ ) contact angles. The maximum value of the surface tension force is obtained

when these limiting angles are reached respectively upstream and downstream of the bubble. Assuming a reasonable variation in contact angle at intermediate points around the circumference of the line of contact, the net surface tension force is [5]

$$F_s = \frac{1}{2} \pi r \sigma \sin \theta_0 (\cos \theta_r - \cos \theta_a). \quad (2)$$

The surface tension force is analogous to the friction force, exactly balancing the resultant of the forces tending to remove the bubble from the surface, until it reaches a maximum value and the bubble moves off into the flow.

#### APPARATUS

Most of the equipment has been described in the previous paper [7]. In fact the measurements of bubble growth and of bubble diameter on departure were performed simultaneously. The only extra items of information needed for the bubble diameter on departure measurements are the advancing and receding contact angles (the equilibrium contact angle was measured on individual bubbles in the test section as explained in the previous paper). The advancing and receding angles were measured using a separate test cell, as shown in Fig. 1(b). A small drop of the liquid from the main test section was placed on a flat plate of the same material and surface condition as that used in the main test section. The plate was tilted until the drop was about to slide down. At this point the limiting contact angles are reached, as shown in Fig. 1(c). A cover to the test cell was found necessary to prevent evaporation of the drop.

#### RESULTS

A sample of the results obtained is shown in Figs. 2-7. Each experimental point is the average of several measurements on different bubbles at a given flow velocity. The theoretical curves drawn are discussed later.

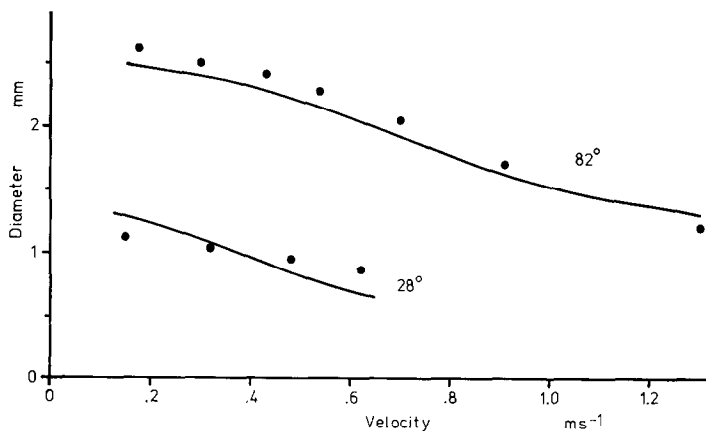


FIG. 5. Results for horizontal flow of ethylene glycol in the 19 mm tubes. The contact angles were: 82, 99.5, 64.5; and 28, 46.5, 9.5.

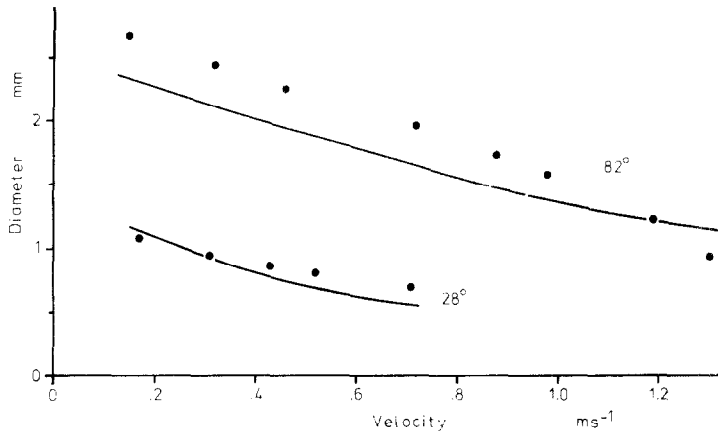


FIG. 6. Results for upward flow of ethylene glycol in the 19 mm tubes. The contact angles were: 82, 99.5, 64.5 and 28, 46.5, 9.5.

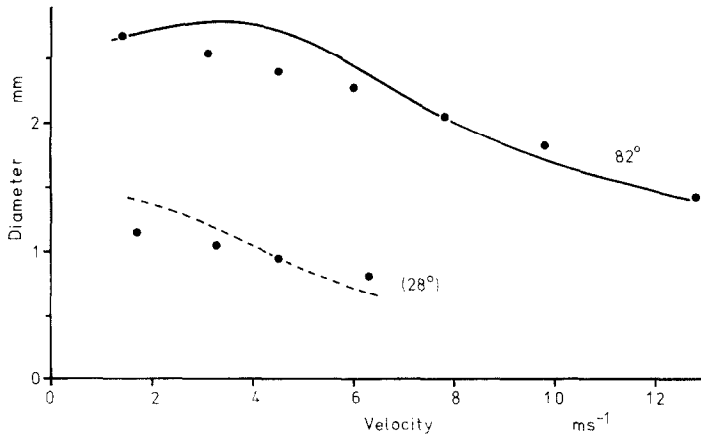


FIG. 7. Results for downward flow of ethylene glycol in the 19 mm tubes. The contact angles were: 82, 99.5, 64.5; and 28, 46.5, 9.5.

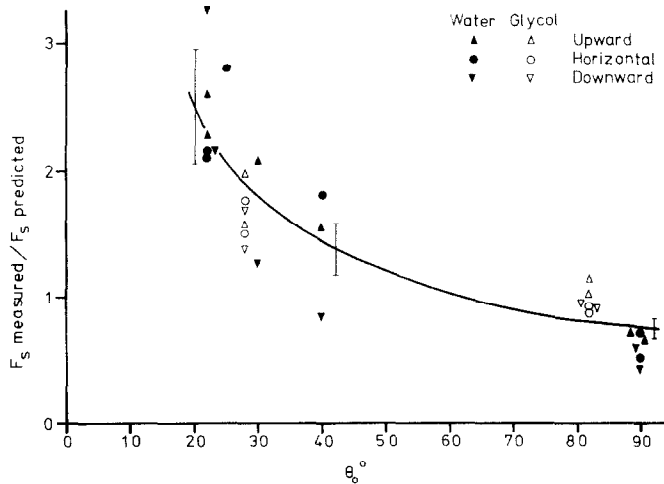


FIG. 8. Ratio of measured surface tension force to that predicted by equation (2).

For water and ethylene glycol measurements were made with all possible combinations of flow direction (horizontal, inclined upward, and inclined downward), tube size (19 and 24 mm dia), and tube material (untreated glass, Perspex and treated glass), with the exception of the ethylene glycol and Perspex combination where a zero contact angle was measured and bubbles would not stick. Otherwise the equilibrium contact angles were fairly low on the untreated glass surface (around 22° for water and 28° for ethylene glycol) slightly higher for the Perspex surface (around 30° for water with more variation from one run to the next), and much higher for the treated glass surface (90° for water and 82° for ethylene glycol).

Measurements were also made using water with detergent, but these have not been analysed in detail because it became clear that the effect of the surface active agent had been to weaken the surface tension force, with the result that these measurements could not be directly compared with those for pure liquids.

The results shown in Figs. 2–7 are for the most part for the 19 mm tubes, since in many ways these results were more interesting than those obtained with the 23 mm tubes. In particular it was possible to obtain a higher range of velocities in the 19 mm tube. Also, as it turned out, the contact angles on the 19 mm Perspex tube tended to be higher, allowing a clearer differentiation between the results for the untreated glass and Perspex surfaces.

Generally the 23 mm tube results were more consistent and in better agreement with the modified theory developed later. For interest Fig. 3 shows one set of measurements on 23 mm diameter tubes, illustrating the overlap of the untreated glass and Perspex results.

Over the whole range, including the water with detergent results, the measurements were in reasonable agreement with the type of analysis described in the theory section, i.e. with the surface tension force given by equation (2) and  $C_d = 18.7/Re_b^{0.68}$ . The measured bubble diameter on detachment was in all cases within a factor of two of the value predicted [8]. To this extent then the results confirm the validity of previous applications of the theory. However we did not feel that the agreement was as good as it might be, particularly since there were clear systematic discrepancies between measurement and prediction, and we had never expected that the drag law would be valid at the larger contact angles. Consequently it was decided to re-analyse the experimental data to provide improved surface tension and drag laws.

#### CALCULATION OF SURFACE TENSION FORCE

For the measurements at the lowest flow velocities the drag force is very small and the bubble diameter largely determined by the surface tension and buoyancy forces. Accordingly the experimental values of bubble diameter were used to calculate the surface tension force at the lowest velocity in each run. The

drag force was estimated using  $C_d = 18.7/Re_b^{0.68}$ , but if the drag force had been omitted altogether or doubled it would only have changed the calculated surface tension force by at most 2%. Since it was known that the surface tension force was given reasonably closely by equation (2) the force calculated from the experimental results was compared with that predicted by the equation (see Fig. 8).

It is clear from Fig. 8 that the equation (2) underestimates the surface tension force at low contact angles and slightly overestimates it at very high contact angles. However, considering that equation (2) contains no empirically derived parameters, the agreement is quite good. The discrepancy between measured and predicted values is no more than might reasonably be expected from distortions in the bubble shape. In particular the variation in contact angle around the line of contact between the bubble and the solid surface is not exactly as assumed in deriving equation (2). Further confirmation that the basic approach used to calculate the surface tension force is correct comes from the error bars shown in the figure. These result from assuming an error of up to 1° in each of the three contact angles. It is not claimed that any of the contact angles were measured with an accuracy of better than 1°, and the advancing and receding values were measured in a separate test cell, not in the main test section. So the spread of data in Fig. 8 is entirely consistent with errors of a couple of degrees in the contact angles. Another satisfactory feature is that the results for water and ethylene glycol lie on essentially the same curve. This is in spite of the fact that the bubble Reynolds numbers for water were typically a factor of ten larger than those for ethylene glycol.

The results for water with added surface active chemical are not included in Fig. 8 because it became clear that they were inconsistent with the results for pure liquids. Measurements were made with 10 ppm by volume of each of the commercial detergents listed in the previous paper, and in each case the surface tension force was very roughly half the value that would have been expected from Fig. 8. This effect is obtained after allowance has been made for the reduced surface tension and changed contact angles.

If the results in Fig. 8 are to be used as the basis of an empirical correction factor for the surface tension force then it is desirable to fit an equation to them. Imposing the conditions that the correction factor should be finite at all contact angles, and decrease steadily with increase in contact angle, the following equation was found to the simplest that gave a reasonable fit.

$$\begin{aligned} & \frac{\text{Measured surface tension force}}{\text{Force predicted from equation (2)}} \\ &= \frac{58}{\theta_0 + 5} + 0.14. \quad (3) \end{aligned}$$

This expression allows for the distortion of the bubble shape. The complete equation for the surface tension force is therefore

$$F_s = \left\{ \frac{58}{\theta_0 + 5} + 0.14 \right\} \times \frac{1}{2} \pi r \sigma \sin \theta_0 (\cos \theta_r - \cos \theta_a) \quad (4)$$

where  $\theta_0$  is in degrees.

#### CALCULATION OF DRAG FORCE

Using equation (4) for the surface tension force an experimental value of the drag coefficient may be calculated for any of the points shown in Figs. 2-7. It quickly became apparent however that there was little to be gained by doing this for the experimental points obtained at low flow velocities. Here the drag force is calculated from the small difference between the surface tension and buoyancy forces. An error of just one or two degrees in the contact angles gives a large error in the surface tension force. The resulting scatter in the  $C_d$  values was very large. Clearly only the measurements at high flow rates where the drag force dominated could be used to obtain reasonable estimates of  $C_d$ . Even here the uncertainty in the surface tension force calculation gave rise to considerable scatter. Fortunately the bubble Reynolds numbers for a given combination of liquid and tube surface showed little variation with flow direction or tube size, so it was possible to work out an average drag coefficient for a given combination of liquid and tube surface. These average values exhibit very little scatter, as may be seen in Fig. 9.

A surprising feature of the results is that over a wide range of Reynolds number the drag coefficient seems to be constant, independent of both Reynolds number and contact angle. At bubble Reynolds numbers below about 20 there is a definite rise in drag coefficient, but again no obvious dependence on contact angle (for these results the simple definition  $Re_b = \rho du/\mu$  is used, with  $d$  the bubble diameter and  $u$  the local velocity at half the distance the bubble projects into the flow).

Over the range as a whole the previously used drag law  $D_d = 18.7/Re_b^{0.68}$  is not too bad an approximation

if a single expression of this type is to be used, but a much closer fit to the experimental results is obtained with a constant  $C_d$  for Reynolds numbers above about 20 and an extension of the Stokes drag law for lower Reynolds numbers. So the recommended expressions for the drag coefficient are:

$$C_d = 1.22 \quad \text{for } 20 < Re_b < 400 \quad (5)$$

and

$$C_d = 24/Re_b \quad \text{for } 4 < Re_b < 20. \quad (6)$$

Equation (6) can probably be used at much lower Reynolds numbers, since it is the theoretical equation for viscous drag on a solid sphere.

#### DISCUSSION

The predicted bubble radius on departure using the new surface tension and drag laws, i.e. equations (4)-(6), is shown as the smooth curve in Figs. 2-7. In the great majority of cases, including all the horizontal and upward flow runs, a good fit is obtained with the measured contact angles. In a small number of cases (shown by dashed lines) it was necessary to bring both advancing and receding contact angles  $2^\circ$  closer to the equilibrium value to get a reasonable fit. This change was considered to be within the likely experimental error. The effect of not making this correction may be seen by comparing Fig. 4 with Fig. 10. In Fig. 10 the measured contact angles are used, giving significant deviations between the predicted and measured values of bubble diameter (the worst of any of the water or ethylene glycol runs).

The fact that these small changes in contact angle are all in the same direction, and confined to the downward flow runs, is not necessarily significant. The change is only  $2^\circ$ , and the results are more sensitive to small changes in the surface tension force when the drag and buoyancy forces are opposed. However, there is another trend in the downward flow results, particularly noticeable in Fig. 10. The predicted diameter

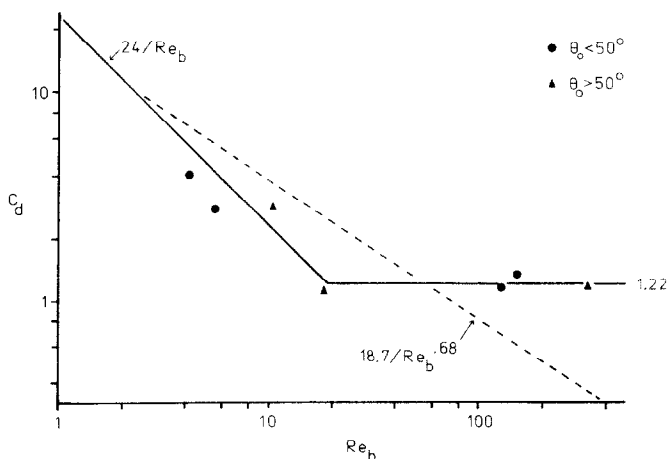


FIG. 9. Drag coefficient calculated from the experimental results as a function of bubble Reynolds number.

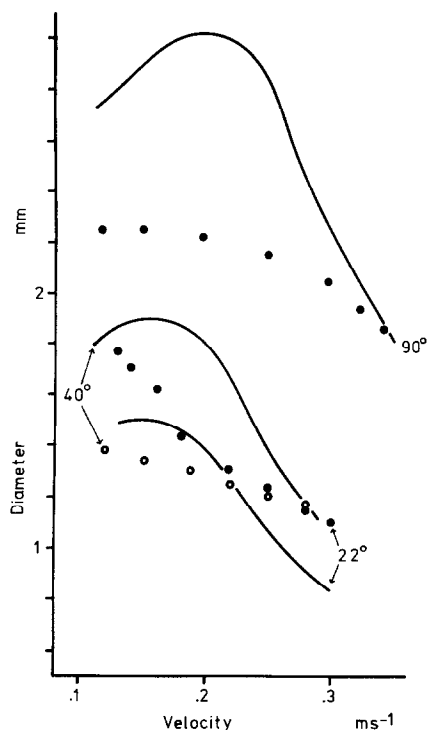


FIG. 10. Results for downward flow of water in the 19 mm tubes, i.e. as Fig. 4 except that the prediction is based on the measured contact angles.

reaches a maximum, whereas the measured values show a steady fall as the flow velocity is increased. It may be that the effect of the two forces acting in opposite directions is to destabilise the bubble, prevent the contact angles reaching the normal limiting values, and reduce the surface tension force. The initial increase in predicted diameter with flow velocity implies incidentally that the bubbles detach against the flow direction at low velocities in downward flow. This was observed experimentally, but the slight initial increase in diameter was not.

If equations (4)–(6) are to be used to make predictions for other situations any inaccuracy in them is

unlikely in practice to be of any importance compared to the difficulty of finding accurate values of the contact angles.

#### CONCLUSIONS

The maximum diameter of gas bubbles adhering to a surface with liquid flowing past can be predicted from the balance of the surface tension, buoyancy and drag forces parallel to the surface.

The expression previously used for the surface tension force is a good first approximation, but better results are obtained with the improved expression, equation (4).

Over a wide range of bubble Reynolds number the drag coefficient calculated from the local flow velocity is essentially constant at 1.22, regardless of contact angle.

The addition of surface active agents can significantly reduce the net surface tension force, over and above the effect to be expected from the reduced value of the surface tension.

*Acknowledgement*—The work described in this paper was supported by a grant from the Science Research Council.

#### REFERENCES

1. R. H. S. Winterton, Effect of gas bubbles on liquid metal heat transfer, *Int. J. Heat Mass Transfer* **17**, 549–554 (1974).
2. A. A. Bishop, F. C. Engel and R. A. Markley, Heat transfer effect of entrained gas in liquid sodium systems, *Nucl. Engng Design* **52**, 1–13 (1979).
3. R. H. S. Winterton, Liquid metal superheat in forced convection, *Int. J. Heat Mass Transfer* **18**, 205–212 (1975).
4. R. H. S. Winterton, A. B. H. Chevalier and G. A. Fowles, Gas bubble adhesion to heat transfer surfaces, *Nucl. Engng Design* **53**, 347–354 (1979).
5. R. H. S. Winterton, Sizes of bubbles produced by dissolved gas, *Chem. Engng Sci.* **27**, 1223–1230 (1972).
6. F. N. Peebles and H. J. Garber, *Chem. Engng Prog.* **49**, 88 (1953).
7. R. A. M. Al-Hayes and R. H. S. Winterton, Bubble growth in flowing liquids, *Int. J. Heat Mass Transfer* **24**, 213–221 (1981).
8. R. A. M. Al-Hayes, Bubble growth and detachment in flowing liquids, Ph.D. Thesis, University of Birmingham (1977).

#### DIAMETRE DES BULLES LORS DU DETACHEMENT DANS LES LIQUIDES EN ECOULEMENT

**Résumé** — Une série de mesures des diamètres de bulles de gaz lors du détachement a été faite pour des liquides en écoulement. Les liquides utilisés sont l'eau, l'eau avec un agent tensioactif et l'éthylène-glycol. Par utilisation de différentes surfaces, les angles de contact varient entre 22 et 90°. A partir de ces résultats, on propose de nouvelles expressions avec la tension superficielle et les forces de traînée pour une bulle attachée à une surface solide.

## DER ABREISSDURCHMESSER VON BLASEN IN STRÖMENDEN FLÜSSIGKEITEN

**Zusammenfassung** — Es wurde eine ausgedehnte Versuchsreihe über den Blasendurchmesser bei der Ablösung in strömenden Flüssigkeiten durchgeführt. Die Versuchsflüssigkeiten waren Wasser, Wasser mit oberflächenaktiven Zusätzen und Äthylenglykol. Durch die Verwendung unterschiedlicher Oberflächen wurden Gleichgewichtsrandwinkel von 22 bis 90° erhalten. Auf der Grundlage dieser Ergebnisse werden neue Beziehungen für die Oberflächenspannungs- und Widerstandskräfte, die von einer Blase auf eine feste Oberfläche ausgeübt werden, vorgeschlagen.

## ОТРЫВНОЙ ДИАМЕТР ПУЗЫРЬКА ПРИ ТЕЧЕНИИ ЖИДКОСТЕЙ

**Аннотация** — Проведена большая серия измерений отрывных диаметров газовых пузырьков при течении ряда жидкостей: воды, смеси воды с поверхностноактивным веществом и этиленгликоля. Благодаря использованию различных поверхностей получены равновесные углы смачивания от 22 до 90°. На основании результатов измерений предложены новые выражения для определения сил поверхностного натяжения и сопротивления, действующих на пузырек на твердой поверхности.